MOLECULAR AND CELLULAR BIOLOGY, Feb. 2004, p. 1628–1639 Vol. 24, No. 4
0270-7306/04/$08.00+0 DOI: 10.1128/MCB.24.4.1628–1639.2004

Actin Cytoskeleton Regulates Calcium Dynamics and NFAT Nuclear Duration

Fabiola V. Rivas, James P. O'Keefe, Maria-Luisa Alegre, and Thomas F. Gajewski*

Department of Pathology, Department of Medicine, and Ben May Institute, The University of Chicago, Chicago, Illinois 60637

Received 19 June 2003/Returned for modification 4 August 2003/Accepted 18 November 2003

T-cell activation by antigen-presenting cells is accompanied by actin polymerization, T-cell receptor (TCR) capping, and formation of the immunological synapse. However, whether actin-dependent events are required for T-cell function is poorly understood. Herein, we provide evidence for an unexpected negative regulatory role of the actin cytoskeleton on TCR-induced cytokine production. Disruption of actin polymerization resulted in prolonged intracellular calcium elevation in response to anti-CD3, thapsigargin, or phorbol myristate acetate plus ionomycin, leading to persistent NFAT (nuclear factor of activated T cells) nuclear duration. These events were dominant, as the net effect of actin blockade was augmented interleukin 2 promoter activity. Increased surface expression of the plasma membrane Ca^{2+} ATPase was observed upon stimulation, which was inhibited by cytochalasin D, suggesting that actin polymerization contributes to calcium export. Our results imply a novel role for the actin cytoskeleton in modulating the duration of Ca^{2+}-NFAT signaling and indicate that actin dynamics regulate features of T-cell activation downstream of receptor clustering.

T-cell activation is triggered by signaling initiated through the T-cell receptor (TCR) and costimulatory molecules, which leads to the production of cytokines such as interleukin 2 (IL-2). The physiological ligand for the TCR is antigenic peptide bound to major histocompatibility complex molecules on the surface of antigen-presenting cells (APCs). Molecular polarization within individual T cells toward APCs has been described by several groups and is one of the initial steps in the formation of the immunological synapse (IS) (5). This cytoskeletal polarization includes the formation of a tight ring of polymerized actin at the contact site as well as the reorientation of the microtubule-organizing center toward the APC.

Whereas the movement of the microtubule-organizing center toward the APC is thought to be involved mainly in the relocalization of the secretory apparatus toward the target cell and directional delivery of effector function, the actin cytoskeleton has been hypothesized to have an important role in signaling to induce T-cell activation (29). Actin polymerization is required for stable conjugate formation between the T cell and the APC as well as for the formation of the highly ordered structures within the IS. These results have suggested that the actin cytoskeleton is important for the stabilization and amplification of T-cell signaling that are implied by the IS hypothesis (18). The phenotypes of T cells that are deficient for molecules implicated in the regulation of actin dynamics initially appeared to provide additional support for this hypothesis. Vav-deficient and Wiskott-Aldrich syndrome protein (WASP)-deficient T cells exhibit defective IL-2 production and are hypoproliferative. $Vav^{-/-}$ T cells also exhibit defects in TCR cap formation, actin polymerization, and formation of a mature IS (12, 13, 22, 33, 35, 38, 40). However, Vav has other functions via its role as a guanine nucleotide exchange factor and through protein-protein interactions, and so the link between actin dynamics and IL-2 production remains correlative. In addition, recent reports have shown no apparent actin polymerization defects in $WASP^{-/-}$ T cells, thus uncoupling the functions of WASP in actin dynamics versus IL-2 production (23). Therefore, a molecular connection between actin polymerization and T-cell activation remains unclear.

An additional role reported for the actin cytoskeleton in T-cell activation is one at the level of costimulation, especially through the molecule CD28. Wulfing and Davis have previously shown that beads attached to the T-cell surface translocate toward the interface between the T cell and the APC, a process which depended on myosin motor proteins and, by inference, the cortical cytoskeleton. Furthermore, they showed that this movement was regulated by CD28/B7 and LFA1-intercellular adhesion molecule 1 interactions, leading to the accumulation of receptor pairs and possibly other signaling molecules in the contact area. They suggested that this aggregation of complexes would result in the amplification of signaling associated with costimulation (39). Others have further shown a CD28-dependent movement of lipid rafts rich in signaling molecules to the interface between the T cell and the APC, and such movement of rafts is thought to be dependent on the actin cytoskeleton (20, 37).

However, other data raise doubts as to whether the actin cytoskeleton and IS formation are necessary for T-cell activation and signal transduction. TCR-induced biochemical responses can be detected prior to the formation of a mature IS, suggesting that the IS is not causal but rather results from T-cell signaling and activation (2, 24). Furthermore, recent reports question the necessity of a stable contact site between the T cell and the APC for T-cell activation (19). In light of these data, we opted to reexamine the role of the actin cytoskeleton in T-cell signal transduction and activation. To this

* Corresponding author. Mailing address: Department of Pathology, Department of Medicine, and Ben May Institute, The University of Chicago, 5841 S. Maryland Ave., MC2115, Chicago, IL 60637. Phone: (773) 702-4601. Fax: (773) 702-3701. E-mail: tgajewsk@medicine.bsd.uchicago.edu.

end, we used the actin polymerization inhibitors cytochalasin D and latrunculin B to determine whether actin polymerization was necessary for specific T-cell functions. Unexpectedly, these manipulations augmented cytokine production by Th1 and Th2 T-cell clones and by DO11.10 or 2C/RAG2$^{-/-}$ TCR transgenic (Tg) T cells in response to anti-CD3- and anti-CD28-coated beads or APCs. This augmentation appeared to be at the level of decreased Ca^{2+} efflux via the plasma membrane calcium ATPase (PMCA), leading to prolonged levels of intracellular Ca^{2+} elevation and prolonged nuclear dwell time of NFAT (nuclear factor of activated T cells). Our results indicate that actin polymerization modulates the duration of TCR-induced Ca^{2+}-NFAT signaling.

MATERIALS AND METHODS

Mice. DBA/2 mice were purchased from the Jackson Laboratory (Bar Harbor, Maine). DO11.10 TCR Tg mice were provided by A. Sperling (University of Chicago, Chicago, Ill.). IL-2 promoter luciferase Tg/DO11.10 mice (referred to as IL-2 luc/DO11.10) were kindly provided by J. Miller (University of Chicago). These mice express the IL-2 promoter region (−590 to +40 bp) upstream of the luciferase gene and were interbred with DO11.10 TCR Tg mice (1). All mice were housed in a specific-pathogen-free barrier facility at the University of Chicago.

Cell lines. Murine Th1 (PGL10 and PGL2) and Th2 (PL104 and PL3) I-A^d-restricted, ovalbumin (OVA)-specific CD4$^+$ T-cell clones were maintained as described previously (17). Before being used in experiments, T cells were purified by centrifugation over Ficoll-Hypaque. Transfectants of the fibrosarcoma cell line 6132-PRO (Pro) expressing I-A^d alone (ProAd) or in combination with B7.1 (ProAd-B7.1) have been described previously (41). ProAd cells were maintained by passage in Dulbecco's modified Eagle's medium (DMEM) supplemented with 10% fetal calf serum (FCS) and G418 (100 μg/ml), and ProAd-B7.1 cells were passaged with 10% FCS, G418 (100 μg/ml), and MXH (6 μg of mycophenolic acid per ml, 250 μg of xanthine per ml, and 15 μg of hypoxanthine per ml).

Jurkat and CEM leukemic cell lines were a kind gift from M. Peter (University of Chicago). Cells were maintained in RPMI culture medium (Gibco) supplemented with 10% FCS, L-glutamine (100 mg/ml), penicillin (100 U/ml), and streptomycin (100 μg/ml).

T-cell stimulations. T cells were stimulated with beads coated with various concentrations of anti-CD3 monoclonal antibody (MAb) (145-2C11) and anti-CD28 MAb (PV1) immobilized to sheep anti-mouse-coated beads (Dynal, Oslo, Norway) as described previously (30). A 5:1 bead-to-T-cell ratio was used. For some experiments, cells were incubated for the indicated length of time at 37°C with the specified concentrations of cytochalasin D or latrunculin B (Calbiochem). For cytokine assays, T cells (10^5) were stimulated either with Ab-coated beads and ProAd-B7.1 cells loaded with OVA peptide (1:1 T-cell-to-APC ratio) or with phorbol myristate acetate (PMA) (50 ng/ml) and ionomycin (0.5 μg/ml) (P+I) in triplicate cultures in 96-well Costar plates (Corning, Cambridge, Mass.) in a final volume of 250 μl. Supernatants were removed at 16 to 24 h and assessed for cytokine content by enzyme-linked immunosorbent assay (ELISA) using Ab pairs obtained from PharMingen (San Diego, Calif.). For biochemical assays, T cells (2.5×10^6) were incubated with Ab-coated beads (12.5×10^6) for various times at 37°C, after which the reaction was stopped by the addition of ice-cold Ca^{2+}- and Mg^{2+}-free Dulbecco's phosphate-buffered saline (DPBS) (Gibco). The cells were then lysed and analyzed by Western blotting.

Confocal microscopy. Analysis of TCR capping was performed as described previously (32). Briefly, PGL10 and PL104 T-cell clones (10^6) were incubated with 5 μg of anti-CD3-fluorescein isothiocyanate (FITC) per ml on ice for 10 min and then stimulated with an equal volume of goat anti-hamster antiserum in culture medium (1:300; prewarmed at 37°C) for 5 min at 37°C in the presence or absence of cytochalasin D. The cells were then fixed in 1% paraformaldehyde, washed, and resuspended in mounting solution (0.5 mg of *o*-phenylenediamine per ml, 90% glycerol, 0.05 M Tris [pH 8.0], 0.2% NaN_3). Images were obtained by using a Fluoview 200 confocal microscope (Olympus, Melville, N.Y.).

Jurkat cells were used for analysis of PMCA expression. The cells were first preincubated with culture medium or cytochalasin D for 1 h at 37°C, followed by addition of P+I. After a 1-h stimulation, cells (5×10^4) were adhered to immunofluorescence slides (Polysciences, Warrington, Pa.) that had been precoated with poly-L-lysine (Sigma, St. Louis, Mo.), fixed and permeabilized with ice-cold methanol-acetone (1:1), and stained as described previously (34). Anti-PMCA Abs 5F10 and JA3 were obtained from Affinity Bioreagents (Golden, Colo.) and Upstate Biotechnologies, respectively. Images were obtained by using a Leica SP2 AOBS confocal microscope (Bannockburn, Ill.). Image analyses were performed using Metamorph (Universal Imaging, Downington, Pa.) and ImageJ.

For IS analysis, APCs were loaded with the vital dye CMAC Cell-Tracker Blue (Molecular Probes, Eugene, Ore.) as previously described (31). APCs (10^5) were mixed with an equal number of Ficoll-Hypaque-purified T cells in DMEM with 10% FCS, centrifuged at 5,000 rpm in an Eppendorf 5415C centrifuge for 30 s, and incubated for the indicated time (minus 2 min) at 37°C. Supernatant was aspirated, and conjugates were then gently resuspended in serum-free DMEM using a 1,000-μl pipetter and plated onto poly-L-lysine (molecular weight, 30,000 to 70,000; Sigma)-coated slides for 2 min before fixation. Slides were fixed in 3% (wt/vol) paraformaldehyde in PBS for 15 min. Samples were permeabilized in 0.3% (vol/vol) Triton X-100 (Sigma) in PBS for 10 min and were then rinsed in PBS and blocked in DMEM containing 10% FCS for 5 min. All subsequent Ab incubations were performed in calcium- and magnesium-free DPBS containing 2% FCS. Primary and secondary Abs were applied sequentially for 60 min at room temperature and washed five times after each incubation with DPBS. After fluorochrome labeling, specimens were mounted in Mowiol 4-88 (Hoechst Celanese, Charlotte, N.C.) with 10% 1,4-diazobicyclo[2.2.2]octane (Sigma) added as an antifade reagent. Samples were analyzed with a Zeiss Axiovert100 microscope. Image capture was performed using SlideBook software (Intelligent Imaging Innovations, Denver, Colo.).

Flow cytometry analysis for intracellular F actin and cytokines. For F-actin staining, PGL10 or PL104 T-cell clones (2×10^6) were pretreated with cytochalasin D or with culture medium for 1 h prior to stimulation. Cells were then stimulated with bead-bound anti-CD3 and anti-CD28 (5:1 bead-to-cell ratio) overnight, harvested, and washed with ice-cold Ca^{2+}- and Mg^{2+}-free DPBS. Cells were fixed with 4% paraformaldehyde, permeabilized, and stained with FITC-phalloidin (1 μg/ml) prior to analysis by flow cytometry. For intracellular IL-2 and gamma interferon (IFN-γ), PGL10 T-cell clones (2×10^6) were pretreated with cytochalasin D or with culture medium for 1 h prior to stimulation. PMA (50 ng/ml) and ionomycin (500 ng/ml) were added for 4 h prior to harvesting. Brefeldin A (1 μg/ml) was added to culture 2 h before harvesting. At the time of harvest, cells were stained with anti-CD4-FITC (Pharmingen) and were then fixed in 4% paraformaldehyde. Cells were then permeabilized in permeabilization buffer (0.3% saponin and 2% FCS in DPBS), followed by staining with either anti-IL-2-phycoerythrin (PE), anti-IFN-γ-PE, or control immunoglobulin-PE conjugate (Pharmingen). After being stained, cells were washed twice in washing buffer (0.03% saponin and 2% FCS in DPBS) and were resuspended in fluorescence-activated cell sorter buffer (2% FCS in DPBS) for analysis by flow cytometry using a FACScan flow cytometer (Becton Dickinson Immunocytometry Systems, Mountain View, Calif.).

Sodium dodecyl sulfate-polyacrylamide gel electrophoresis (SDS-PAGE), immunoprecipitation, and immunoblotting. Unless otherwise indicated, the lysis buffer consisted of 50 mM Tris-HCl (pH 7.6), 5 mM EDTA, 150 mM NaCl, 1 mM Na_3VO_4, 10 μg of leupeptin per ml, 10 μg of aprotinin per ml, 10 μg of soybean trypsin inhibitor per ml, 1 mM benzamidine, 25 mM *p*-nitrophenyl *p*-guanidinebenzoate, 1 mM phenylmethylsulfonyl fluoride, 1 mM sodium fluoride (pH 7.4), and 0.5% Triton X-100. Cells were lysed for 30 min on ice, after which the lysates were centrifuged for 10 min at 14,000 rpm in an Eppendorf 5415C centrifuge. The supernatants were then transferred to a new tube containing 5× reducing sample buffer (250 mM Tris-HCl [pH 6.8], 500 mM dithiothreitol [DTT], 10% SDS, 50% glycerol, 0.5% bromophenol blue, 2% β-mercaptoethanol). Samples were heated for 5 min at 95°C and loaded onto an SDS–10% polyacrylamide gel. After transferring the samples onto a polyvinylidene difluoride membrane (Millipore, Bedford, Mass.), we performed Western blotting with Abs from the following sources: anti-phospho-extracellular signal-regulated kinase (ERK) and anti-phospho-c-Jun N-terminal kinase (JNK) (Promega, Madison, Wis.); anti-JNK1 MAb (PharMingen); anti-ERK MAb (Zymed, South San Francisco, Calif.); anti-phosphotyrosine MAb 4F10 (Upstate Biotechnologies); anti-ZAP-70 and anti-TCRζ (Santa Cruz Biotechnology); anti-PMCA (5F10; Affinity Bioreagents); and anti-PMCA4b (JA3; Upstate Biotechnologies).

Immunoprecipitations were performed as described previously (11). The lysate was transferred onto Protein A beads coated with anti-phosphotyrosine Ab (clone FB2, kindly provided by A. Sperling). After an overnight incubation at 4°C, immunoprecipitated proteins were eluted from the protein A beads by the addition of 5× reticulocyte standard buffer and boiling for 5 min at 95°C, and immunoprecipitates were analyzed by Western blotting as described above.

Semiquantitative RT-PCR. PGL10 cells were stimulated with bead-bound anti-CD3 and anti-CD28 for 6 h at 37°C. Total RNA was isolated by phenol-chloroform extraction, and 3 μg was used for first-strand cDNA synthesis. cDNA

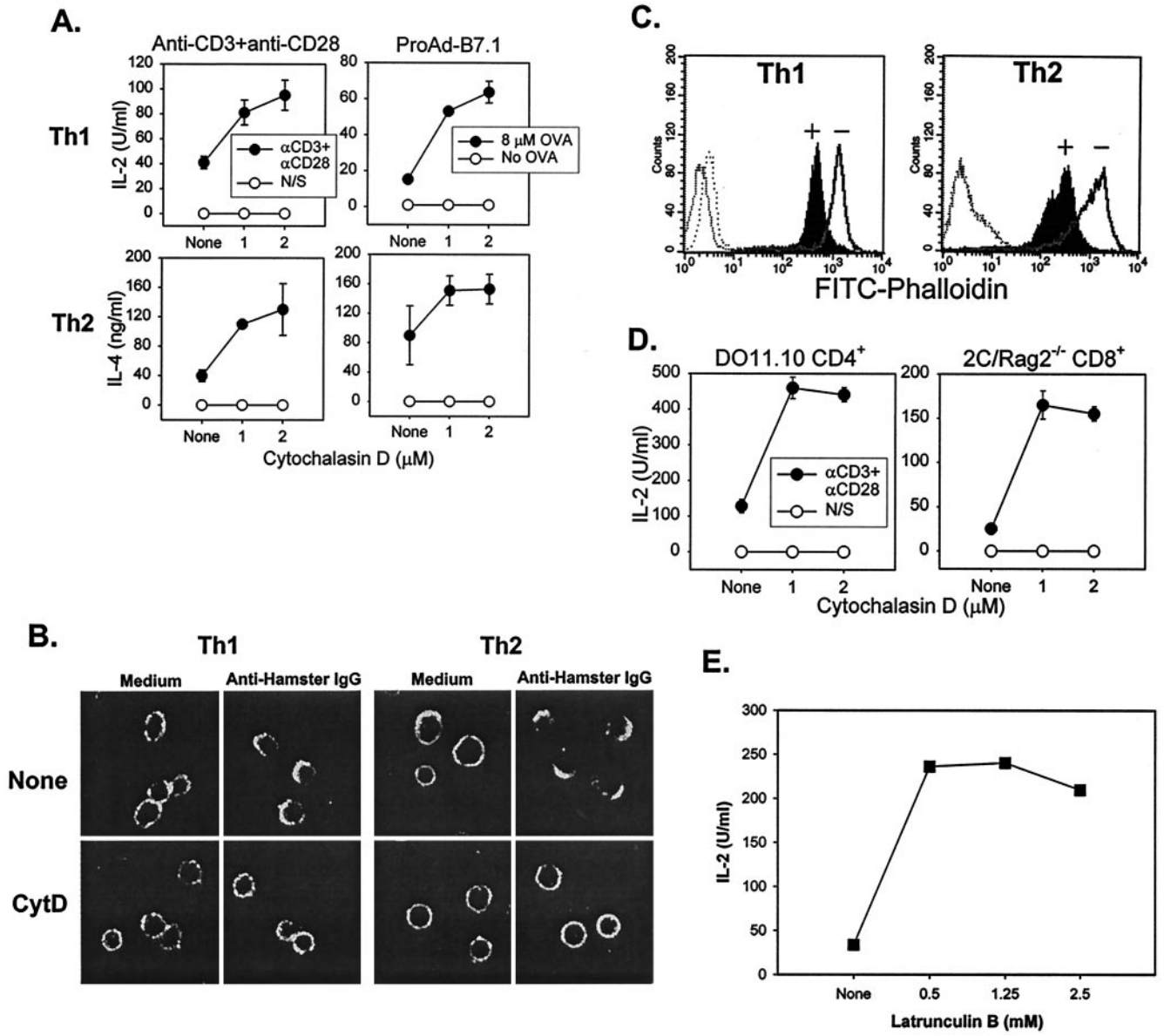

FIG. 1. Cytochalasin D augments cytokine production by Th1 and Th2 T-cell clones and by $CD4^+$ and $CD8^+$ TCR Tg T cells. (A) Cytokine production by Th1 and Th2 T-cell clones is augmented by cytochalasin D treatment. Th1 (PGL10) and Th2 (PL104) T-cell clones were incubated with culture medium or with the indicated concentrations of cytochalasin D for 1 h at 37°C prior to stimulation with bead-bound Abs or APCs. Anti-CD3 (1 μg/ml) and anti-CD28 (1 μg/ml) were used for Ab stimulation, and a 5:1 bead-to-cell ratio was used. The fibrosarcoma cell line 6132A-Pro transfected with I-Ad and B7.1 (ProAd-B7.1) was used as an APC population. Mitomycin C-treated ProAd-B7.1 cells pulsed with OVA peptide (8 μM) were used at a stimulator-to-responder ratio of 1:1. After 16 h at 37°C, cytokine production was measured by ELISA. (B) Cytochalasin D inhibits TCR capping for both Th1 and Th2 clones. Th1 and Th2 T-cell clones were incubated with either culture medium or cytochalasin D for 1 h, followed by the addition of anti-CD3-FITC and a 45-min incubation on ice. Anti-CD3 was cross-linked by adding goat anti-hamster antiserum, followed by a 5-min incubation at 37°C. The cells were then fixed and analyzed by confocal microscopy. IgG, immunoglobulin G. (C) Levels of polymerized actin are decreased by cytochalasin D treatment. T cells were incubated for 16 h with culture medium (solid line, unfilled peak labeled "−") or with cytochalasin D (2 μM) (solid line, filled peak labeled "+"). Levels of F actin were detected by intracellular staining with FITC-phalloidin followed by flow cytometry. Unstained T cells, both treated and untreated (dotted lines), are shown as controls. (D) Cytochalasin D augments IL-2 production by ex vivo DO11.10 $CD4^+$ T cells and 2C/$RAG2^{-/-}$ $CD8^+$ T cells. T cells were purified and incubated with culture medium or the indicated concentrations of cytochalasin D for 1 h at 37°C prior to stimulation with bead-bound Abs as described for panel A. After 16 h at 37°C, IL-2 production was measured by ELISA. (E) Latrunculin B also augments cytokine production. pGL10 cells were stimulated with anti-CD3- and anti-CD28-coated beads in the presence of increasing concentrations of latrunculin B. IL-2 production was measured after 16 h by ELISA.

samples were serially diluted (fivefold dilutions) and analyzed by semiquantitative reverse transcriptase PCR (RT-PCR) by using primers specific for IL-2 (BioSource), β-actin, or hypoxanthine guanine phosphoribosyl transferase. PCR products were visualized on a 1% ethidium bromide-stained agarose gel.

IL-2-Luc/DO11.10 T-cell activation and measurement of luciferase activity. $CD4^+$ T cells were isolated from spleen by using a negative-enrichment protocol based on a magnetic separation system (Stem Cell Technologies, Vancouver, British Columbia, Canada). $CD4^+$ D011.10 and IL-2-Luc/DO11.10 T cells were primed by stimulation with DBA/2 splenocytes. Purified $CD4^+$ T cells (10^5) from DO11.10 or IL-2-luc/DO11.10 mice were cocultured with irradiated DBA/2

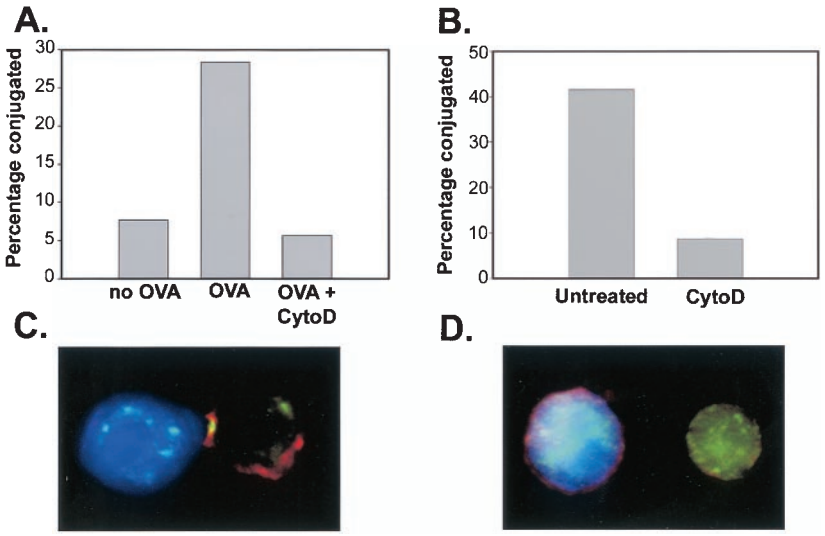

FIG. 2. Cytochalasin D (CytoD) disrupts stable T-cell and APC conjugates and the IS. (A) PGL10 T-cell clones were cocultured with ProAD-B7.1 cells in the presence or absence of OVA peptide either in the presence or absence of cytochalasin D for 30 min. Two-color flow cytometric analysis was performed, and percent conjugates were determined by calculating the ratio of double-positive cells to the total T-cell population. 2C effector $CD8^+$ T cells and P815-B7.1 cells were cocultured for 10 min either in the presence or absence of cytochalasin D (panels B through D). The percentage of T cells conjugated was determined as described above (B). Representative images are shown for the absence (C) or presence (D) of cytochalasin D in T cells and APCs.

splenocytes (0.5×10^6; 2,000 rad) and OVA (200 μg/ml) in 24-well Linbro tissue culture plates (ICN Biomedicals, Emeryville, Calif.). After 7 days in culture, cells were harvested and purified by centrifugation over Ficoll-Hypaque for use in experiments.

IL-2-Luc/DO11.10 T cells (2×10^6) were incubated for 1 h with culture medium or cytochalasin D prior to stimulation with anti-CD3- and anti-CD28-coated beads (5:1 bead-to-cell ratio) or with ProAd-B7.1 cells (1:1 T-cell-to-APC ratio). Cells were stimulated for 16 h, after which they were harvested and washed with ice-cold Ca^{2+}- and Mg^{2+}-free DPBS. Cells were then lysed (0.5% NP-40, 100 mM KPO_4 [pH 7.8], 1 mM DTT), and luciferase activity was quantified as described previously (26).

Transcription factor translocation assays. Detection of transcription factors in nuclear and cytoplasmic fractions was performed as described previously (9). Briefly, 2×10^6 T cells were stimulated in the presence or absence of cytochalasin D either with P+I or with anti-CD3- and anti-CD28-coated beads for the specified time periods. The cells were then lysed (0.05% NP-40, 10 mM HEPES [pH 7.9], 10 mM KCl, 0.1 mM EDTA, 0.5 mM phenylmethylsulfonyl fluoride, 1.5 μg of aprotinin per ml, 1 μg of leupeptin per ml, 1 mM DTT, 1 mM NaF), and nuclear and cytosolic fractions were separated by centrifugation (5,000 rpm, Eppendorf 5415C centrifuge, 5 min). Cytosolic fractions were further purified by high-speed centrifugation (40,000 rpm, Beckman OPTIMA LE-80K centrifuge, 1 h). Nuclear fractions were vortexed in a high-salt-content buffer (20 mM HEPES [pH 7.9], 0.4 M NaCl, 1 mM EDTA, 1 mM phenylmethylsulfonyl fluoride, 1.5 μg of aprotinin per ml, 1 μg of leupeptin per ml, 1 mM DTT, 1 mM NaF) for 1 h at 4°C, followed by centrifugation (14,000 rpm, Eppendorf 5415C centrifuge, 5 min). Nuclear and cytoplasmic fractions were then treated with 5× reticulocyte standard buffer, boiled at 95°C for 5 min, and analyzed by SDS-PAGE, which was followed by Western blotting. Abs to NFATc1, NFATc2, phospho-c-Jun, phospho-Elk-1, lamin A, and lamin B were obtained from Santa Cruz Biotechnology.

Calcium flux assays. PGL10 T-cell clones (4×10^6) were loaded with FuraRed (80 μg/ml) and Fluo-3AM (8 μg/ml) (Molecular Probes) for 30 min at 37°C in cell loading buffer (1% FCS in Hanks' buffered saline solution [Gibco]), followed by washing with 5% FCS culture medium. The cells were then incubated with culture medium or cytochalasin D (2 μM) for 1 h at 37°C, after which cells were stimulated with either P+I or thapsigargin (Calbiochem), and Ca^{2+} mobilization was measured by flow cytometry using an LSR flow cytometer (Becton Dickinson). Cell events were recorded for at least 10 min, and analysis was performed using FlowJo software. An increase in the FL1/FL3 fluorescence ratio was indicative of an increase in the Ca^{2+} ion level. For stimulation with anti-CD3 MAb, cells were loaded with dyes as described above, followed by incubation with anti-CD3 (5 μg/ml) on ice for 10 min; the cells were then stimulated with an equal volume of goat anti-hamster antiserum in culture medium (1:300; prewarmed to 37°C) in the presence or absence of cytochalasin D.

Conjugate formation. The conjugate formation assay was performed similarly as described previously (28). Briefly, T cells were labeled with calceinAM (Molecular Probes), and target cells were labeled with PKH (Sigma). T cells (2.5×10^5) and targets (5×10^5) were mixed, centrifuged, lightly vortexed, and incubated at 37°C for the indicated times. Cells were then vortexed vigorously for 30 s and immediately fixed. Two-color flow cytometric analysis was performed, and percent conjugates were determined by calculating the ratio of double-positive conjugates to the total number of T cells.

RESULTS

Cytochalasin D augments cytokine production by Th1 and Th2 T-cell clones and by $CD4^+$ and $CD8^+$ TCR Tg T cells. Although actin-dependent clustering of the TCR occurs following receptor ligation, whether actin polymerization is required for TCR-induced function in normal T cells is not formally known. To address this question, we stimulated OVA-specific $CD4^+$ Th1 and Th2 T-cell clones with beads that were coated with anti-CD3 and anti-CD28 MAbs in the presence of increasing doses of the actin polymerization inhibitor cytochalasin D, and cytokine production was measured by ELISA. As shown in Fig. 1A, cytochalasin D treatment augmented IL-2 production by Th1 T cells and IL-4 production by Th2 cells. Similar results were observed for other Th1 (IFN-γ) and Th2 (IL-5 and IL-10) cytokines (data not shown). Cytochalasin D also augmented cytokine production in response to OVA peptide-pulsed APCs that had been engineered to express the appropriate class II major histocompatibility complex ($I\text{-}A^d$) and B7-1 (Fig. 1A). Similar results were observed with an additional Th1 and Th2 T-cell clone (data not shown).

To confirm that the cytochalasin D used was having the expected inhibitory effect on actin dynamics, TCR capping occurring in Th1 and Th2 T-cell clones was assessed by confocal microscopy. As anticipated, cytochalasin D treatment

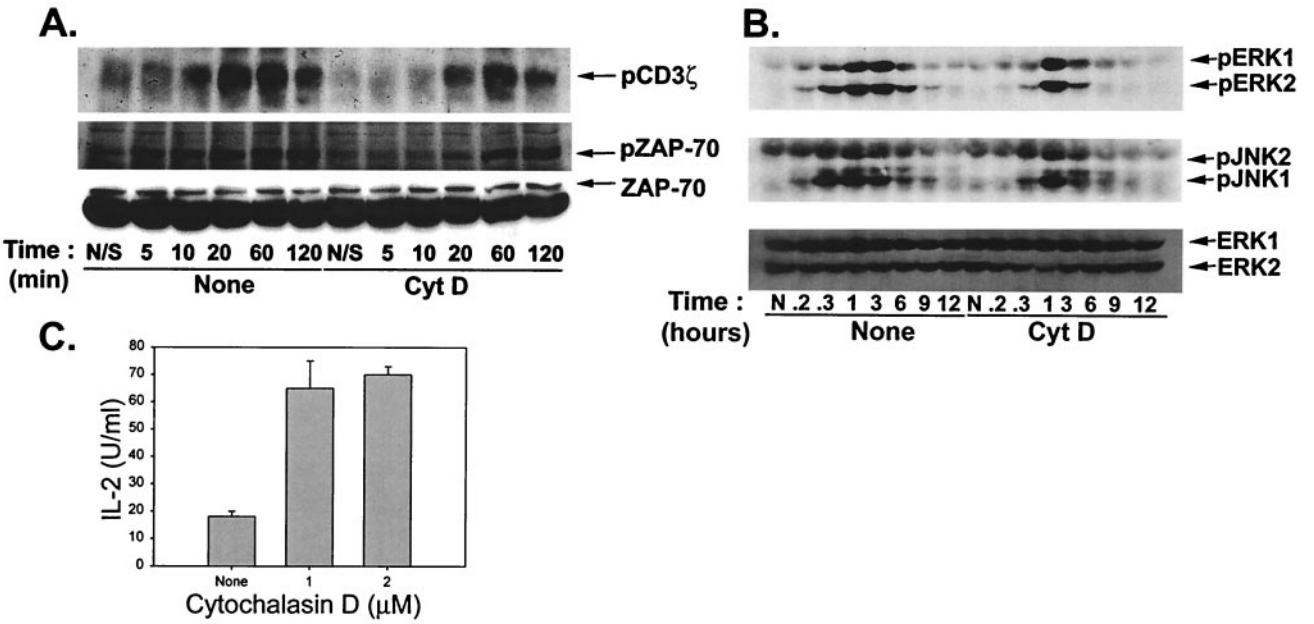

FIG. 3. Cytochalasin D (CytD) does not act by augmenting proximal TCR signaling. (A) Cytochalasin D treatment blunts TCR-proximal signaling. Th1 T cells were incubated with either culture medium or cytochalasin D (2 μM) for 1 h at 37°C prior to stimulation with bead-bound anti-CD3 plus anti-CD28 MAbs for the indicated times. After stimulation, cells were lysed and analyzed by Western blotting with anti-phosphotyrosine MAb for detection of phosphorylated ZAP-70 or else were subjected to immunoprecipitation with anti-phosphotyrosine supernatant (FB2) for analysis of TCRζ chain phosphorylation. Immunoprecipitates were analyzed by SDS-PAGE followed by Western blotting with anti-phosphotyrosine MAb (4F10). (B) Signaling through the MAPK pathways is delayed and blunted by cytochalasin D treatment. Th1 T cells were incubated with either culture medium or cytochalasin D (2 μM) for 1 h at 37°C prior to stimulation with anti-CD3 plus anti-CD28 MAbs for the indicated times. After stimulation, cells were lysed and lysates were analyzed by SDS-PAGE followed by Western blotting with Abs specific for phospho-ERK and phospho-JNK. Equivalent loading of cell lysates was confirmed by blotting for total ERK1/2. (C) IL-2 production by Th1 T-cell clones stimulated with P+I is augmented by cytochalasin D treatment. Th1 T cells were incubated with culture medium or the indicated concentrations of cytochalasin D, followed by addition of P+I. After 16 h at 37°C, IL-2 production was assayed by ELISA.

prevented receptor clustering (Fig. 1B). Similarly, F-actin content as assessed by intracellular staining with FITC-Phalloidin was prevented by cytochalasin D (Fig. 1C), and cell proliferation was diminished as measured by thymidine incorporation (data not shown). We also tested whether disruption of the actin cytoskeleton similarly affected cytokine production by ex vivo TCR Tg $CD4^+$ and $CD8^+$ T cells. As shown in Fig. 1D, cytochalasin D augmented IL-2 production by $CD4^+$ DO11.10 and $CD8^+$ 2C/$RAG2^{-/-}$ Tg T cells stimulated with bead-bound anti-CD3 and anti-CD28 MAbs. To determine whether this phenomenon was unique to cytochalasin D, a second actin polymerization inhibitor, latrunculin B, was utilized. Cytokine production by Th1 cells (Fig. 1E) and Th2 cells (data not shown) was also potentiated by latrunculin B. Thus, contrary to expectations, disruption of the actin cytoskeleton potentiated rather than inhibited cytokine production by normal murine T-cell populations.

It was of interest to analyze stable T-cell-APC conjugate formation and IS generation in the presence of cytochalasin D in order to determine whether these processes were dispensable for cytokine production. In fact, stable conjugate formation between Th1 cells and OVA-pulsed ProAd.B7-1 cells as assessed by flow cytometry was disrupted by cytochalasin D (Fig. 2A). This occurred despite the fact that the same conditions potentiated cytokine production (Fig. 1A). Similar results were seen with primed 2C $CD8^+$ TCR Tg T cells interacting with P815.B7-1 target cells (Fig. 2B). Stable conjugates were also not observed by confocal microscopy in the presence of cytochalasin D; therefore, assessment of the IS was not possible. As represented in Fig. 2C, the T-cell-APC contact site was normally characterized by peripheral talin staining and central PKCθ staining, hallmarks of the pSMAC and cSMAC, respectively (14). However, in the presence of cytochalasin D, only individual cells were observed (Fig. 2D). Collectively, these results suggest that durable conjugate formation and IS generation (at least at a detectable level) are not mandatory for T-cell cytokine production in response to APCs.

Cytochalasin D does not act by augmenting proximal TCR signaling. The increase in cytokine production observed in the presence of cytochalasin D could theoretically have occurred at any of several levels, from potentiation of proximal TCR signaling through facilitation of protein secretion. To begin to dissect the mechanism of this effect, Th1 T-cell clones were stimulated with anti-CD3 and anti-CD28 MAbs, and the phosphorylation status of specific substrates was examined. In the absence of cytochalasin D, phosphorylation of the TCRζ chain was detectable by 5 min, peaked between 20 and 60 min, and showed some decay at 2 h poststimulation (Fig. 3A). However, in the presence of cytochalasin D, TCRζ chain phosphorylation occurred with delayed kinetics and at a decreased magnitude. Similar results were observed with phosphorylation of ZAP-70 (Fig. 3A). The effect of cytochalasin D on mitogen-activated protein kinase (MAPK) activation was also assessed. As shown in Fig. 3B, phosphorylation of both ERK and JNK in

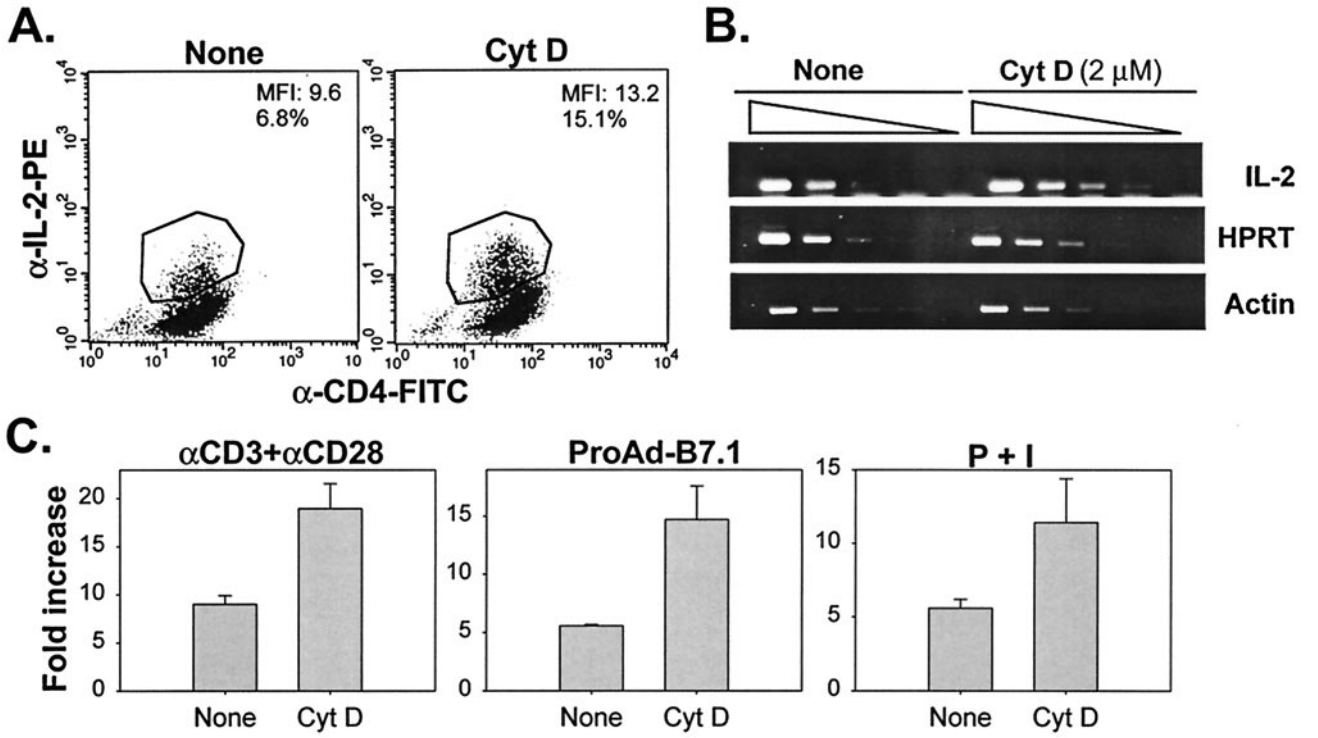

FIG. 4. The increase in IL-2 production by cytochalasin D (CytD) is reflected at the level of IL-2 gene transcription. (A) Cytochalasin D increases cytokine production at the intracellular protein level. Th1 cells were incubated with culture medium or cytochalasin D (2 μM) for 1 h prior to stimulation with P+I. Cells were stimulated for 4 h at 37°C. Two hours prior to harvesting, brefeldin A was added to the samples. Cells were stained as indicated, and intracellular cytokine levels were determined by flow cytometry. (B) Cytochalasin D treatment increases steady-state IL-2 mRNA levels. Th1 T-cell clones were stimulated with bead-bound anti-CD3 plus anti-CD28 MAbs for 6 h at 37°C in the presence or absence of cytochalasin D. Total RNA was isolated by phenol-chloroform extraction and used for first-strand cDNA synthesis. cDNA samples were serially diluted and analyzed by semiquantitative RT-PCR using IL-2 primers. RT-PCRs for β-actin and hypoxanthine guanine phosphoribosyl transferase (HPRT) were performed as controls for mRNA abundance. (C) IL-2 promoter activity is augmented upon cytochalasin D treatment. IL-2-Luc/DO11.10 T cells were incubated for 1 h with culture medium or cytochalasin D prior to stimulation with anti-CD3- and anti-CD28-coated beads, ProAd-B7.1 cells, or P+I. Cells were stimulated for 16 h, after which they were harvested, lysed, and assayed for luciferase activity.

response to TCR-CD28 ligation was similarly blunted and delayed in the presence of cytochalasin D. Similar results were seen for Th2 T-cell clones (data not shown).

To determine whether cytokine production was potentiated by cytochalasin D even under conditions in which proximal TCR signaling was not involved, stimulation was performed with P+I. Unexpectedly, cytochalasin D treatment also augmented IL-2 production in response to P+I (Fig. 3C), suggesting that the effect is distal from TCR oligomerization and proximal signaling events. A parallel implication of these results is that cytokine production can clearly occur with less than maximal phosphorylation of TCRζ, ZAP70, ERK, and JNK.

Increase in IL-2 production by cytochalasin D is reflected at the level of IL-2 gene transcription. To determine whether the potentiation of detectable IL-2 release in the presence of cytochalasin D was reflected at the level of increased IL-2 protein synthesis, we assayed for intracellular cytokine levels. In fact, a greater percentage of positive cells and mean fluorescence intensity of IL-2 staining was observed upon stimulation in the presence of cytochalasin D (Fig. 4A).

We asked next whether augmentation by cytochalasin D was detectable at the level of steady-state mRNA abundance. $CD4^+$ Th1 T cells were stimulated with anti-CD3 and anti-CD28 MAbs for 4 h in the absence or presence of cytochalasin D, after which time cDNA was obtained and analyzed by semiquantitative RT-PCR. Th1 T cells treated with cytochalasin D showed approximately three- to fivefold-increased levels of IL-2 mRNA (Fig. 4B). Furthermore, this increase was at the level of transcription of the IL-2 gene, as DO11.10 T cells Tg for a luciferase reporter under control of the IL-2 promoter exhibited augmented luciferase activity upon cytochalasin D treatment (Fig. 4C). This was true whether the cells were stimulated with anti-CD3- and anti-CD28-coated beads, APCs pulsed with OVA, or P+I. Similar results were obtained with latrunculin B (data not shown). Thus, disruption of the actin cytoskeleton results in increased IL-2 gene transcription, with an overall outcome of increased IL-2 protein, detected both intracellularly and in culture supernatants.

Disruption of the actin cytoskeleton results in prolonged NFAT nuclear duration. The augmentation of IL-2 gene expression by cytochalasin D prompted examination of transcription factors that are thought to be important for IL-2 gene transcription. To this end, an assay was developed to separate nuclear from cytosolic fractions to monitor the translocation of proteins to the nucleus poststimulation. As shown in Fig. 5A, Western blot analysis for lamin A and IκB kinase β confirmed that T-cell nuclear and cytosolic fractions were appropriately isolated, and the purity of these fractions was not affected by

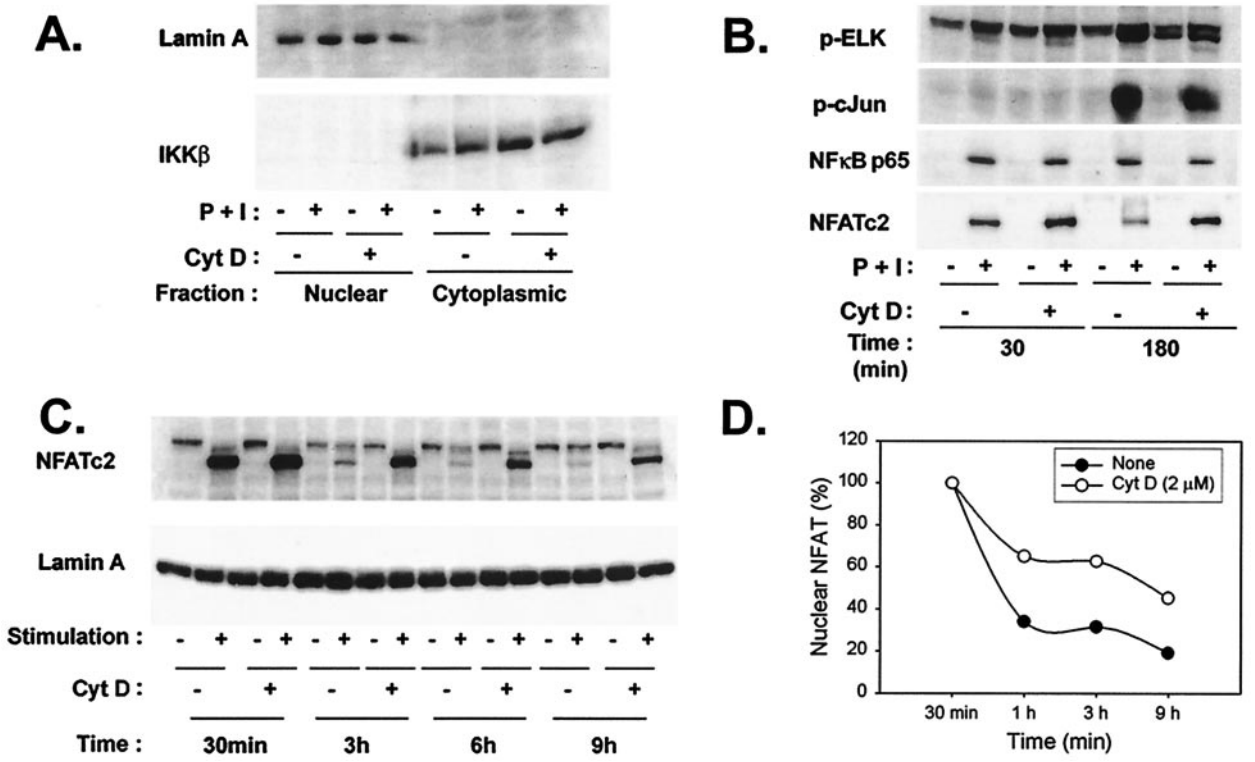

FIG. 5. Disruption of the actin cytoskeleton results in prolonged NFAT nuclear duration. (A) Separation of nuclear and cytoplasmic fractions is not affected by stimulation or cytochalasin D (CytD) treatment. Th1 cells incubated with culture medium or cytochalasin D (2 μM) for 1 h at 37°C were left either unstimulated or stimulated with P+I for the indicated periods. Cells were then lysed, and nuclear and cytoplasmic fractions obtained. Fractions were analyzed by Western blotting for the presence of the indicated proteins. IKKβ, IκB kinase β. (B) Cytochalasin D treatment results in increased nuclear localization of NFAT but not of other transcription factors relevant to IL-2 production. Th1 T-cell clones were incubated with culture medium or cytochalasin D and were then stimulated with P+I for the indicated times. Nuclear lysates were obtained and analyzed for the presence of the indicated transcription factors by Western blotting. (C) NFAT nuclear localization is prolonged by cytochalasin D. Th1 cells were incubated with culture medium or cytochalasin D, as described above, and were then stimulated with P+I for the indicated times. Presence of NFATc2 in the nucleus was determined by Western blotting of nuclear lysates. The blot was then stripped and reprobed for lamin A as an equivalent loading control. (D) The dephosphorylated NFAT bands shown in panel C were quantified by densitometry analysis. NFAT levels in both untreated and cytochalasin D-treated samples at 30 min were assigned a starting value of 100%, the intensities of all bands were compared to these values, and the percentage of nuclear NFAT in both sets of samples was calculated accordingly.

the presence of cytochalasin D. Consistent with the decreased phosphorylation of ERK and JNK observed in the presence of cytochalasin D, detection of phosphorylated forms of the target transcription factors Elk-1 and c-Jun in the nucleus at 180 min poststimulation was diminished (Fig. 5B). Similarly, inducible translocation of NF-κB p65 was modestly decreased by cytochalasin D. In contrast, nuclear accumulation of NFATc2 was augmented in the presence of cytochalasin D. Similar results were seen for NFATc1 (data not shown). Kinetic experiments were performed in order to further characterize this augmentation. It is striking that increased nuclear levels of NFATc2 were observed at all time points beyond 30 min in stimulated T cells treated with cytochalasin D (Fig. 5C and D). Similar results were observed in Th2 T-cell clones (data not shown). Thus, interference with actin polymerization results in prolonged NFAT nuclear duration.

Nuclear export of NFAT is not affected by cytochalasin D. Prolonged nuclear presence of NFAT may result from decreased nuclear export or persistent nuclear translocation. Export of NFAT is thought to be mediated via phosphorylation by GSK3, the activity of which is diminished by phosphorylation following T-cell stimulation (6). As shown in Fig. 6A, GSK3 phosphorylation induced during T-cell stimulation was not altered by cytochalasin D. To more directly determine the effect on NFAT export, Th1 T-cell clones were stimulated with P+I for 3 h either in the absence or presence of cytochalasin D. At this time, cyclosporine A was added to inhibit further nuclear entry of NFAT, and amounts of nuclear NFAT through time were determined by Western blotting. The dose of cyclosporine A used completely inhibited IL-2 production (data not shown). As shown in Fig. 6B, more nuclear NFAT was detected in T cells treated with cytochalasin D at the initial time of addition of cyclosporine A. However, the rate of decay of detectable nuclear NFATc2 in the nucleus was comparable with or without cytochalasin D. The half-life of nuclear NFAT was approximately 30 min whether cells were stimulated in the presence or absence of cytochalasin D (Fig. 6C). These results imply that the prolonged nuclear duration of NFATc2 is likely a consequence of persistent nuclear translocation rather than of decreased export.

Prolonged elevation of intracellular calcium levels upon disruption of actin cytoskeleton. As persistent translocation of NFAT to the nucleus would likely result from prolonged du-

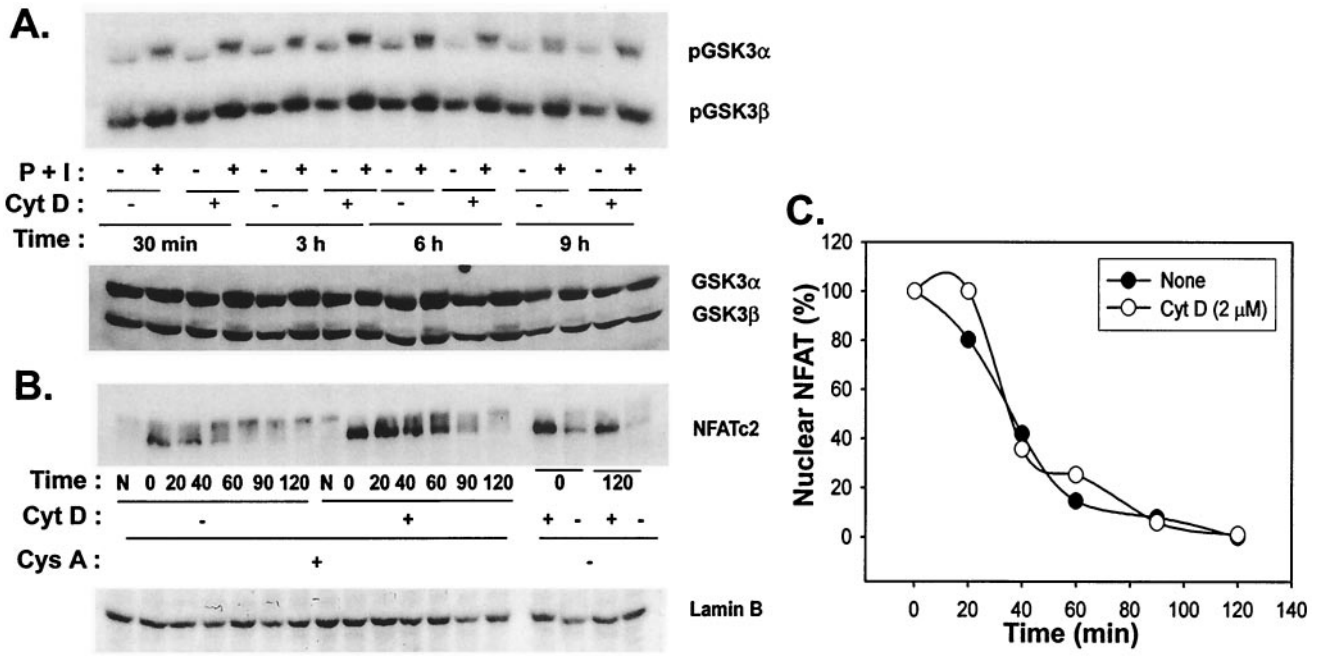

FIG. 6. Nuclear export of NFAT is not affected by cytochalasin D (CytD). (A) Cytochalasin D does not affect inactivation of GSK-3. Th1 T-cell clones were incubated with culture medium or cytochalasin D for 1 h at 37°C and were then stimulated with P+I for the indicated times. Cells were lysed and analyzed for inactivation of GSK-3 by Western blotting with a phospho-GSK3 MAb. Blots were stripped and reprobed for GSK3α/β to verify equivalent loading of cell lysates. (B) The rate of NFAT nuclear export is unaffected by cytochalasin D. Th1 cells were incubated with culture medium or cytochalasin D, as described above and were then stimulated with P+I for 3 h at 37°C, at which time cyclosporine A (Cys A) (50 ng/ml) was added as indicated. Time zero is defined as the time of addition of cyclosporine A. Stimulation of samples was continued for the indicated times, after which cells were harvested and lysed. Cell lysates were separated into nuclear and cytoplasmic fractions, and the presence of NFATc2 in the nucleus was assessed by Western blotting. (C) Quantification of rate of export of nuclear NFAT. The dephosphorylated NFAT bands shown in panel B were quantified by densitometry analysis. NFAT levels in both untreated and cytochalasin D-treated samples at the time of addition of cyclosporine A were assigned a starting value of 100%, the intensities of all bands were compared to these values, and the percentage of nuclear NFAT in both sets of samples was calculated accordingly.

ration of intracellular calcium concentration, the dynamics of calcium flux were assessed by flow cytometry in the presence or absence of cytochalasin D. As shown in Fig. 7A, the rate of decay of calcium levels was diminished in the presence of the drug, although the peak intracellular calcium concentration induced by CD3 cross-linking was comparable with or without cytochalasin D. We asked whether Ca^{2+} flux that initiated independent of ligation of the TCR would show similar characteristics upon cytochalasin D treatment. To this end, Th1 T-cell clones were stimulated with thapsigargin, treatment with which results in increased cytosolic Ca^{2+} levels by blocking the endoplasmic reticulum Ca^{2+} ATPase. As shown in Fig. 7B, cytochalasin D treatment prolonged elevated levels of intracellular Ca^{2+} in Th1 cells that had been stimulated with thapsigargin. Finally, to induce calcium entry into the cells directly, stimulation with P+I was utilized. Interestingly, cytochalasin D similarly blunted the rate of decay of intracellular calcium in response to P+I (Fig. 6C). Again, the peak Ca^{2+} flux was similar in both treated and untreated samples. When the results of five similar experiments were quantitated, the difference between the slope of decay and the total Ca^{2+} flux area under the curve in the presence of cytochalasin D was significant ($P < 0.05$, paired t test).

Cytochalasin D decreases localization of the PMCA to the plasma membrane. That cytochalasin D slowed the rate of decay of intracellular Ca^{2+} in response to a calcium ionophore, which should mediate direct calcium entry, suggested that Ca^{2+} clearance from the cell was likely being affected. Although the mechanism of Ca^{2+} efflux from lymphocytes is not completely understood (25), PMCA has been shown to be involved with Jurkat T cells (4). We hypothesized that T-cell stimulation would increase the function of the PMCA in an actin-dependent fashion. The most straightforward mechanism envisioned was that T-cell signaling would induce relocalization of the PMCA to the plasma membrane and that this relocalization would be blocked by cytochalasin D.

The available MAbs against PMCA recognized the human form and did not recognize a specific band in mouse T-cell lysates by Western blotting (data not shown). Therefore, Jurkat T cells were utilized as a model to examine the cellular localization of the PMCA by confocal microscopy. As shown in Fig. 8A, staining with anti-PMCA MAb revealed a patchy diffuse distribution within the cell, consistent with presence in vesicles, with little plasma membrane localization. Western blot analysis revealed that the total levels of PMCA were constant with or without 1-h stimulation with P+I and also in the presence of cytochalasin D (Fig. 8B). However, stimulation with P+I resulted in increased PMCA staining intensity at the plasma membrane, consistent with membrane translocation, and this redistribution was not observed in the presence of

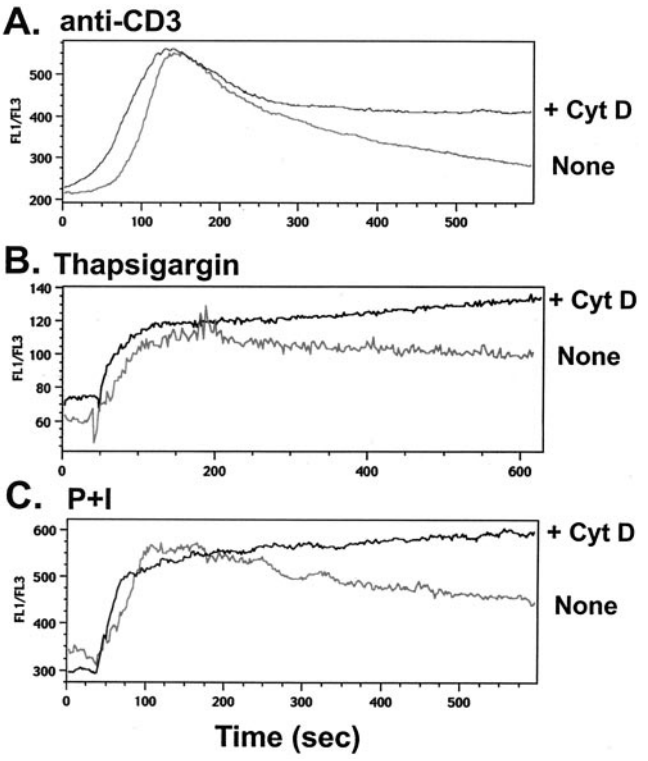

FIG. 7. Prolonged elevation of intracellular calcium upon disruption of the actin cytoskeleton. (A) Cytochalasin D (CytD) treatment prolongs Ca^{2+} flux in T cells stimulated with anti-CD3 MAb. Th1 T-cell clones were labeled with Ca^{2+} binding dyes FuraRed and Fluo3, followed by incubation with culture medium or cytochalasin D (2 μM) for 1 h at 37°C. Cells were then incubated for 1 h on ice with 5 μg of anti-CD3 MAb per ml. Cells were then warmed to 37°C, and Ca^{2+} flux was measured by flow cytometry after the addition of goat anti-hamster antiserum. (B) Ca^{2+} flux is prolonged by cytochalasin D in T cells stimulated with thapsigargin. Th1 T cells were labeled as described above and incubated with culture medium or cytochalasin D for 1 h at 37°C. Cells were then stimulated with thapsigargin, and Ca^{2+} flux was measured. (C) Cytochalasin D prolongs elevated levels of intracellular Ca^{2+} in T cells stimulated with P+I. Labeled Th1 T cells were incubated with culture medium or cytochalasin D for 1 h at 37°C. Ca^{2+} flux was measured following the addition of P+I.

cytochalasin D (Fig. 8C). Quantitation of membrane versus cytosolic staining intensity over a cohort of imaged cells revealed significant inhibition by cytochalasin D ($P < 0.05$ by unpaired *t* test; Fig. 8D). Consistent with the functional outcome observed for mouse T cells, cytochalasin D treatment augmented IL-2 production by Jurkat T cells stimulated with P+I (Fig. 8E). Similar results were seen with another human T-cell leukemia CEM (data not shown). These results support a model in which calcium efflux via the PMCA is facilitated by an actin-dependent mechanism that is blocked with cytochalasin D.

DISCUSSION

We used the actin polymerization inhibitors cytochalasin D and latrunculin B to address the effect of disruption of actin dynamics in T-cell activation. Contrary to expectations, cytokine production was potentiated by cytochalasin D treatment in T cells stimulated with anti-CD3- and CD28-coated beads, antigen-loaded APCs, or P+I. Our findings thus uncouple the requirement for a dynamic actin cytoskeleton for cytokine production in $CD4^+$ and $CD8^+$ T cells. At first glance, our data are in conflict with previous reports that show decreased cytokine production upon inhibition of actin polymerization (22, 36). We believe that at least part of the discrepancy is due to the different methods of stimulation used. Holsinger et al. stimulated Jurkat T cells with plate-bound anti-CD3 MAb, whereas we utilized bead-bound Abs, APCs, and P+I. Interestingly, we have been able to reproduce the inhibitory effect of cytochalasin D on cytokine production by using plate-bound anti-CD3 plus anti-CD28 MAbs (data not shown), thereby arguing that this form of stimulation does not mimic the interaction between T cells and APCs. In part, this result may be accounted for by a failure of the T cells to adhere to the Ab-coated plate in the presence of cytochalasin D.

Actin cytoskeleton and signal stabilization. Analysis of TCR-proximal and MAPK pathways revealed that duration of signaling as reflected by protein phosphorylation was blunted upon cytochalasin D treatment, a finding that supports a role for the actin cytoskeleton in signal stabilization. The mechanism by which the actin cytoskeleton would participate in maintaining antigen receptor signaling is unclear. It has been suggested that it may serve as a scaffold to which signaling molecules would bind and thus be protected from degradation by proteosomal pathways. This idea has some similarity to the spatial segregation model proposed by the IS hypothesis, in which the highly ordered structures at the SMAC result in the separation of phosphatases from kinases and their phosphorylated substrates (5, 29, 36). Another hypothesis is that a critical mass of signaling molecules may be created through actin-mediated aggregation and that this resulting complex would be

FIG. 8. Cytochalasin D (CytD) decreases localization of the PMCA to the plasma membrane. (A) Anti-PMCA Ab stains an intracellular protein. Jurkat cells were permeabilized and stained with either FITC anti-mouse alone (left) or with anti-PCMA followed by FITC anti-mouse (right). Images were obtained by confocal microscopy. The upper and lower panels are representative of the cells imaged. (B) Protein levels of PMCA are not affected by P+I or cytochalasin D. Jurkat T cells were either unstimulated, stimulated with P+I, or stimulated with P+I along with cytochalasin D for 1 h. Cells were lysed and analyzed for PMCA expression by Western blotting. (C) Decreased localization of PMCA to the plasma membrane after P+I stimulation upon treatment with cytochalasin D. Jurkat T cells were preincubated with culture medium or cytochalasin D for 1 h at 37°C and were left either unstimulated or stimulated with P+I for 1 h. Cells were then fixed, permeabilized, and stained, followed by analysis for PMCA (upper panels) or giantin (lower panels) expression by confocal microscopy. (D) Quantitation of levels of PMCA staining in the plasma membrane versus those in the cytosol in untreated versus cytochalasin D-treated cells. Imaging software was used to quantify fluorescence intensity of PMCA-stained samples in the cytosol and plasma membrane. The mean ratio of plasma membrane to cytosol fluorescence intensity of nine cells per sample is shown. (E) Cytochalasin D increases IL-2 production by Jurkat T cells. Jurkat T cells were preincubated with culture medium or cytochalasin D, followed by stimulation with P+I. After 16 h, levels of IL-2 in the supernatant were measured by ELISA.

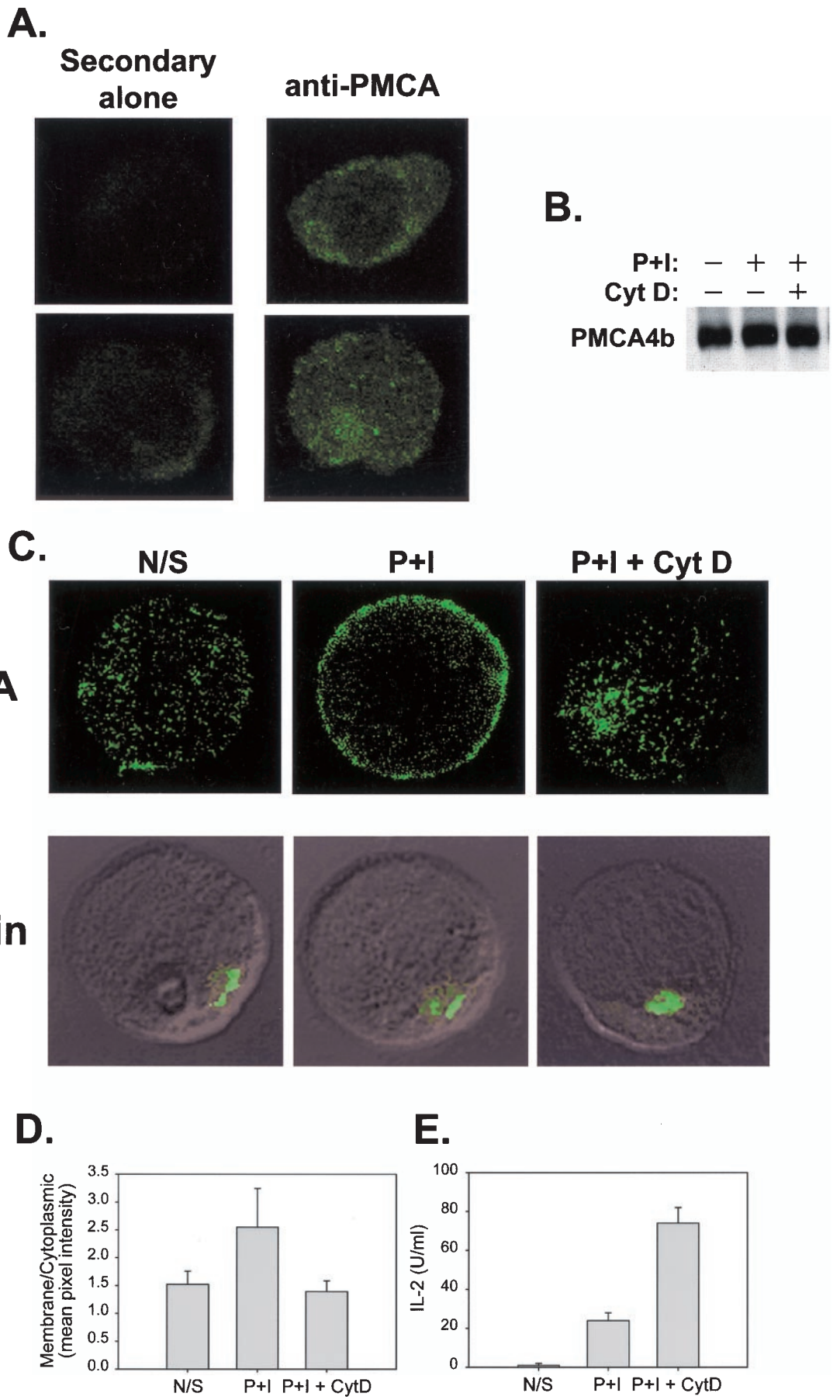
A.
Secondary alone
anti-PMCA
B.
P+I: – + +
Cyt D: – – +
PMCA4b
C.
N/S
P+I
P+I + Cyt D
PMCA
Giantin
D.
Membrane/Cytoplasmic (mean pixel intensity)
3.5
3.0
2.5
2.0
1.5
1.0
0.5
0.0
N/S
P+I
P+I + CytD
E.
IL-2 (U/ml)
100
80
60
40
20
0
N/S
P+I
P+I + CytD

able to maintain signaling for increased periods. However, more evidence is necessary to substantiate these ideas.

It is noteworthy that we were able to detect cytokine production with less than maximal phosphorylation of TCRζ, ZAP70, ERK, JNK, and the transcription factors c-Jun and Elk-1. Our data suggest that these lower levels are sufficient for cytokine production. The fact that we were able to detect increased cytokine production in this setting, which correlated with increased NFAT nuclear localization, argues for the importance of signal integration at the level of transcription factor assembly. Thus, reduced levels of NKκB, c-Jun, and Elk-1 (and by inference, AP-1), in combination with the increased level of NFAT, actually resulted in augmented IL-2 promoter activity. These results argue for a cumulative signal that commits T cells to IL-2 gene transcription.

Regulation of the PMCA by actin dynamics. Our results suggest that the localization of the PMCA can be regulated by the actin cytoskeleton in T cells. PMCA is also regulated by Ca^{2+}/calmodulin binding, and by PKC, facts which at least partially explain PMCA's increased activity upon T-cell activation (3, 4, 10). We observed increased PMCA staining at the plasma membrane upon T-cell stimulation, and this was inhibited by treatment with cytochalasin D. This decreased plasma membrane expression correlated with slower decay of intracellular Ca^{2+} following T-cell stimulation in the presence of cytochalasin D. Of note, these increased levels of intracellular Ca^{2+} were physiologically meaningful, as they correlated with prolonged presence of NFAT in the nucleus and increased cytokine production upon disruption of the actin cytoskeleton.

Though our findings suggest that the actin cytoskeleton has a net negative impact on T-cell activation, a more complex relationship may exist. PMCA activity has been proposed to enhance the stability of Ca^{2+} signaling by adjusting the efflux rate to match influx through the calcium release-activated calcium channel (4). This clearance may be necessary for proper T-cell activation, as persistent elevated levels of intracellular Ca^{2+} and persistent nuclear localization of NFAT have been associated with B- and T-cell anergy (15, 16, 21, 27). Moreover, studies have shown that different Ca^{2+} signaling patterns can activate distinct transcriptional pathways in T cells, implying that cells can extract meaningful information from the amplitude and frequency of Ca^{2+} spikes (7, 8). Our data add to this complexity by showing a role for the actin cytoskeleton in Ca^{2+} dynamics with a clear impact on NFAT nuclear duration and transcriptional activity. We propose that the actin cytoskeleton contributes to regulating levels of intracellular Ca^{2+}, at least in part, through modulation of PMCA surface expression and thus participates in the interpretation of signals mediated by Ca^{2+}-responsive pathways. To speculate that PMCA inhibitors might be able to promote T-cell tolerance by prolonging intracellular Ca^{2+} levels and generating an anergic state is tempting.

Although we have shown that the augmentative effect of cytochalasin D on T-cell cytokine production is correlated with increased IL-2 promoter activity, our results do not exclude additional effects downstream from transcription, such as those on the levels of mRNA stability, protein translation, and cytokine secretion. Nonetheless, the increased IL-2 promoter activity may be sufficient to explain this phenomenon.

In summary, we describe herein a novel aspect of regulation of T-cell activation by the actin cytoskeleton. Our results are consistent with those of a model in which an actin-dependent increase in plasma membrane localization of the PMCA contributes to efficient Ca^{2+} efflux and restoration of intracellular Ca^{2+} levels to a resting state. Further work will be necessary to characterize the precise contribution of the PMCA to T-cell regulation at the molecular level.

ACKNOWLEDGMENTS

We are grateful to J. Miller, A. Sperling, A. Lin, and M. Peter for providing mice and reagents, and we thank B. Eisfelder, V. Bindokas, P. E. Fields, and H. Harlin for experimental advice. We also thank J. Washington and E. Marshall for technical assistance.

This work was supported by NIH grant number R01 AI47919.

REFERENCES

1. **Abraham, C., and J. Miller.** 2001. Molecular mechanisms of IL-2 gene regulation following costimulation through LFA-1. J. Immunol. **167:**5193–5201.
2. **Acuto, O., and D. Cantrell.** 2000. T cell activation and the cytoskeleton. Annu. Rev. Immunol. **18:**165–184.
3. **Balasubramanyam, M., and J. P. Gardner.** 1995. Protein kinase C modulates cytosolic free calcium by stimulating calcium pump activity in Jurkat T cells. Cell Calcium **18:**526–541.
4. **Bautista, D. M., M. Hoth, and R. S. Lewis.** 2002. Enhancement of calcium signalling dynamics and stability by delayed modulation of the plasma-membrane calcium-ATPase in human T cells. J. Physiol. **541:**877–894.
5. **Bromley, S. K., W. R. Burack, K. G. Johnson, K. Somersalo, T. N. Sims, C. Sumen, M. M. Davis, A. S. Shaw, P. M. Allen, and M. L. Dustin.** 2001. The immunological synapse. Annu. Rev. Immunol. **19:**375–396.
6. **Crabtree, G. R., and E. N. Olson.** 2002. NFAT signaling: choreographing the social lives of cells. Cell **109**(Suppl.)**:**S67–S79.
7. **Dolmetsch, R. E., R. S. Lewis, C. C. Goodnow, and J. I. Healy.** 1997. Differential activation of transcription factors induced by Ca^{2+} response amplitude and duration. Nature **386:**855–858.
8. **Dolmetsch, R. E., K. Xu, and R. S. Lewis.** 1998. Calcium oscillations increase the efficiency and specificity of gene expression. Nature **392:**933–936.
9. **Dong, C., D. D. Yang, M. Wysk, A. J. Whitmarsh, R. J. Davis, and R. A. Flavell.** 1998. Defective T cell differentiation in the absence of Jnk1. Science **282:**2092–2095.
10. **Enyedi, A., A. K. Verma, R. Heim, H. P. Adamo, A. G. Filoteo, E. E. Strehler, and J. T. Penniston.** 1994. The Ca^{2+} affinity of the plasma membrane Ca^{2+} pump is controlled by alternative splicing. J. Biol. Chem. **269:**41–43.
11. **Fields, P. E., and T. F. Gajewski.** 2000. Biochemical analysis of activated T lymphocytes. Protein phosphorylation and Ras, ERK, and JNK activation. Methods Mol. Biol. **134:**307–317.
12. **Fischer, K. D., Y. Y. Kong, H. Nishina, K. Tedford, L. E. Marengere, I. Kozieradzki, T. Sasaki, M. Starr, G. Chan, S. Gardener, M. P. Nghiem, D. Bouchard, M. Barbacid, A. Bernstein, and J. M. Penninger.** 1998. Vav is a regulator of cytoskeletal reorganization mediated by the T-cell receptor. Curr. Biol. **8:**554–562.
13. **Fischer, K. D., A. Zmuldzinas, S. Gardner, M. Barbacid, A. Bernstein, and C. Guidos.** 1995. Defective T-cell receptor signalling and positive selection of Vav-deficient $CD4^+$ $CD8^+$ thymocytes. Nature **374:**474–477.
14. **Freiberg, B. A., H. Kupfer, W. Maslanik, J. Delli, J. Kappler, D. M. Zaller, and A. Kupfer.** 2002. Staging and resetting T cell activation in SMACs. Nat. Immunol. **3:**911–917.
15. **Gajewski, T. F., P. Fields, and F. W. Fitch.** 1995. Induction of the increased Fyn kinase activity in anergic T helper type 1 clones requires calcium and protein synthesis and is sensitive to cyclosporin A. Eur. J. Immunol. **25:**1836–1842.
16. **Gajewski, T. F., D. W. Lancki, R. Stack, and F. W. Fitch.** 1994. "Anergy" of TH0 helper T lymphocytes induces downregulation of TH1 characteristics and a transition to a TH2-like phenotype. J. Exp. Med. **179:**481–491.
17. **Gajewski, T. F., M. Pinnas, T. Wong, and F. W. Fitch.** 1991. Murine Th1 and Th2 clones proliferate optimally in response to distinct antigen-presenting cell populations. J. Immunol. **146:**1750–1758.
18. **Grakoui, A., S. K. Bromley, C. Sumen, M. M. Davis, A. S. Shaw, P. M. Allen, and M. L. Dustin.** 1999. The immunological synapse: a molecular machine controlling T cell activation. Science **285:**221–227.
19. **Gunzer, M., A. Schafer, S. Borgmann, S. Grabbe, K. S. Zanker, E. B. Brocker, E. Kampgen, and P. Friedl.** 2000. Antigen presentation in extracellular matrix: interactions of T cells with dendritic cells are dynamic, short lived, and sequential. Immunity **13:**323–332.
20. **Harder, T., and K. Simons.** 1999. Clusters of glycolipid and glycosylphosphatidylinositol-anchored proteins in lymphoid cells: accumulation of actin regulated by local tyrosine phosphorylation. Eur. J. Immunol. **29:**556–562.

21. **Healy, J. I., R. E. Dolmetsch, L. A. Timmerman, J. G. Cyster, M. L. Thomas, G. R. Crabtree, R. S. Lewis, and C. C. Goodnow.** 1997. Different nuclear signals are activated by the B cell receptor during positive versus negative signaling. Immunity **6:**419–428.
22. **Holsinger, L. J., I. A. Graef, W. Swat, T. Chi, D. M. Bautista, L. Davidson, R. S. Lewis, F. W. Alt, and G. R. Crabtree.** 1998. Defects in actin-cap formation in Vav-deficient mice implicate an actin requirement for lymphocyte signal transduction. Curr. Biol. **8:**563–572.
23. **Krawczyk, C., A. Oliveira-dos-Santos, T. Sasaki, E. Griffiths, P. S. Ohashi, S. Snapper, F. Alt, and J. M. Penninger.** 2002. Vav1 controls integrin clustering and MHC/peptide-specific cell adhesion to antigen-presenting cells. Immunity **16:**331–343.
24. **Lee, K. H., A. D. Holdorf, M. L. Dustin, A. C. Chan, P. M. Allen, and A. S. Shaw.** 2002. T cell receptor signaling precedes immunological synapse formation. Science **295:**1539–1542.
25. **Lewis, R. S.** 2001. Calcium signaling mechanisms in T lymphocytes. Annu. Rev. Immunol. **19:**497–521.
26. **Liu, Z. G., H. Hsu, D. V. Goeddel, and M. Karin.** 1996. Dissection of TNF receptor 1 effector functions: JNK activation is not linked to apoptosis while NF-κB activation prevents cell death. Cell **87:**565–576.
27. **Macian, F., F. Garcia-Cozar, S. H. Im, H. F. Horton, M. C. Byrne, and A. Rao.** 2002. Transcriptional mechanisms underlying lymphocyte tolerance. Cell **109:**719–731.
28. **Morgan, M. M., C. M. Labno, G. A. Van Seventer, M. F. Denny, D. B. Straus, and J. K. Burkhardt.** 2001. Superantigen-induced T cell:B cell conjugation is mediated by LFA-1 and requires signaling through Lck, but not ZAP-70. J. Immunol. **167:**5708–5718.
29. **Penninger, J. M., and G. R. Crabtree.** 1999. The actin cytoskeleton and lymphocyte activation. Cell **96:**9–12.
30. **Rivas, F. V., S. O'Herrin, and T. F. Gajewski.** 2001. CD28 is not required for c-Jun N-terminal kinase activation in T cells. J. Immunol. **167:**3123–3128.
31. **Sedwick, C. E., M. M. Morgan, L. Jusino, J. L. Cannon, J. Miller, and J. K. Burkhardt.** 1999. TCR, LFA-1, and CD28 play unique and complementary roles in signaling T cell cytoskeletal reorganization. J. Immunol. **162:**1367–1375.
32. **Smith, J. A., Q. Tang, and J. A. Bluestone.** 1998. Partial TCR signals delivered by FcR-nonbinding anti-CD3 monoclonal antibodies differentially regulate individual Th subsets. J. Immunol. **160:**4841–4849.
33. **Snapper, S. B., F. S. Rosen, E. Mizoguchi, P. Cohen, W. Khan, C. H. Liu, T. L. Hagemann, S. P. Kwan, R. Ferrini, L. Davidson, A. K. Bhan, and F. W. Alt.** 1998. Wiskott-Aldrich syndrome protein-deficient mice reveal a role for WASP in T but not B cell activation. Immunity **9:**81–91.
34. **Stegh, A. H., B. C. Barnhart, J. Volkland, A. Algeciras-Schimnich, N. Ke, J. C. Reed, and M. E. Peter.** 2002. Inactivation of caspase-8 on mitochondria of Bcl-x_L-expressing MCF7-Fas cells: role for the bifunctional apoptosis regulator protein. J. Biol. Chem. **277:**4351–4360.
35. **Tarakhovsky, A., M. Turner, S. Schaal, P. J. Mee, L. P. Duddy, K. Rajewsky, and V. L. Tybulewicz.** 1995. Defective antigen receptor-mediated proliferation of B and T cells in the absence of Vav. Nature **374:**467–470.
36. **Valitutti, S., M. Dessing, K. Aktories, H. Gallati, and A. Lanzavecchia.** 1995. Sustained signaling leading to T cell activation results from prolonged T cell receptor occupancy. Role of T cell actin cytoskeleton. J. Exp. Med. **181:**577–584.
37. **Viola, A., S. Schroeder, Y. Sakakibara, and A. Lanzavecchia.** 1999. T lymphocyte costimulation mediated by reorganization of membrane microdomains. Science **283:**680–682.
38. **Wulfing, C., A. Bauch, G. R. Crabtree, and M. M. Davis.** 2000. The vav exchange factor is an essential regulator in actin-dependent receptor translocation to the lymphocyte-antigen-presenting cell interface. Proc. Natl. Acad. Sci. USA **97:**10150–10155.
39. **Wulfing, C., and M. M. Davis.** 1998. A receptor/cytoskeletal movement triggered by costimulation during T cell activation. Science **282:**2266–2269.
40. **Zhang, R., F. W. Alt, L. Davidson, S. H. Orkin, and W. Swat.** 1995. Defective signalling through the T- and B-cell antigen receptors in lymphoid cells lacking the vav proto-oncogene. Nature **374:**470–473.
41. **Zuckerman, L. A., A. J. Sant, and J. Miller.** 1995. Identification of a unique costimulatory activity for murine T helper 1 T cell clones. J. Immunol. **154:**4503–4512.